Applied Radiation and Isotopes 199 (2023) 110874

Contents lists available at ScienceDirect

Applied Radiation and Isotopes

journal homepage: www.elsevier.com/locate/apradiso

Investigation of dosimetric properties of $CaSO_4$:Mn phosphor prepared using slow evaporation route

Anderson M.B. Silva [a,*], Daniel S. Rodrigues [a], Patrícia L. Antonio [b], Danilo O. Junot [c], Linda V.E. Caldas [b], Divanizia N. Souza [a]

[a] Departamento de Física, Universidade Federal de Sergipe, Marechal Rondon, S/N, 49100-000, São Cristovão, SE, Brazil
[b] Instituto de Pesquisas Energéticas e Nucleares, Comissão Nacional de Energia Nuclear, IPEN/CNEN-SP, Av. Prof. Lineu Preste, 2242, 05508-000, São Paulo, SP, Brazil
[c] Instituto de Física Armando Dias Tavares, Universidade do Estado do Rio de Janeiro UERJ, Rua São Francisco Xavier, 524, 20550-013, Rio de Janeiro, RJ, Brazil

ARTICLE INFO

Keywords:
Dosimetric properties
Slow evaporation route
Thermoluminescence
Optically stimulated luminescence
$CaSO_4$: Mn

ABSTRACT

The objective of this work was to investigate the luminescent properties of $CaSO_4$:Mn synthesized by slow evaporation route. The crystalline structure, morphology, thermal and optical properties of the phosphors were characterized by X-ray diffraction analysis (XRD), Scanning electron microscopy (SEM), photoluminescence (PL) and thermogravimetric analysis (TGA). Moreover, using thermoluminescence (TL) and optically stimulated luminescence (OSL) techniques, the dosimetric properties of the phosphors, such as emission spectra, glow curve reproducibility, dose-response linearity, fading of the luminescent signal, variation of the TL intensity with the heating rate, OSL decay curves, correlation between TL and OSL emissions and minimum detectable dose (MDD) were comprehensively investigated. For dosimetric analyses, the samples were irradiated with doses from 169 mGy to 10 Gy. The emission band fits with the characteristic line of the Mn^{2+} emission features, ascribed to $^6A_1 \rightarrow {}^4T_1$ transition. $CaSO_4$:Mn pellets present a TL glow curve with a single typical peak centered around 494 nm, an OSL decay curve with predominance of a fast decay component, and a MDD on the order of mGy. The luminescent signals showed to be linear and reproducible in the studied dose range. The trapping centers located between 0.83 eV and 1.07 eV were revealed for different heating rates in the TL study. The high TL sensitivity of $CaSO_4$:Mn was proven when comparing with commercially available dosimeters. The luminescent signals exhibit a smaller fading than described in the literature for $CaSO_4$:Mn produced by other methods.

1. Introduction

Manganese divalent (Mn^{2+}) ions are significant transition metal activators for broadband and wavelength-tunable luminescence due to the d-d electronic transitions and the interactions with 3 d^5 electronic configuration (Liu et al., 2017).

In recent decades, these ions have attracted considerable attention due to their applications in many technological fields, such as in biomedical imaging and labelling (Song et al., 2015), magnetic sensors (Raghuwanshi et al., 2014), displays (Wang et al., 2014), lasers (Du et al., 2021), photovoltaic applications (Zhou et al., 2015) and optical data storage (Lin et al., 2020). Moreover, the development and study of luminescence of synthetic materials subsidized with manganese ions for radiation dosimetry application have been for many years investigated and are still intensively researched, primarily for use in thermoluminescent (TL) and optically stimulated luminescent (OSL) dosimetry (Bahl et al., 2017; Luchechko et al., 2019; Menon et al., 2005; Oberhofer and Scharmann 1993; Yamashita et al., 1970; Zahedifar et al., 2011).

From the host material point of view, calcium sulphate ($CaSO_4$) activated with manganese was the first investigated synthetic material to be used as thermally stimulated luminescence dosimeter (Bahl et al., 2017). Despite this fact, $CaSO_4$:Mn attracted attention because of its outstanding sensitivity (Watanabe 1951); its use was limited due to a simple reason that its TL glow curve presented a single peak centered at 100 °C and considerable fading of the TL signal (40–85% in the first 3 days after the irradiation) (Oberhofer and Scharmann 1993).

For the purpose of expanding the supply of viable solid-state detectors, a large number of methods were commonly used for the preparation of $CaSO_4$ powders, such as the co-precipitation method (Nuraeni et al., 2019), recrystallization method (Bahl et al., 2017), sol-gel method (Kadari et al., 2016), hydrothermal method (Zahedifar et al., 2011), solid state reaction route (Rani et al., 2015) and slow evaporation route

* Corresponding author.
E-mail address: andersonmanoel22@hotmail.com (A.M.B. Silva).

https://doi.org/10.1016/j.apradiso.2023.110874
Received 6 December 2022; Received in revised form 3 April 2023; Accepted 24 May 2023
Available online 25 May 2023

(Yamashita et al., 1970).

Thereby, according to the antecedents mentioned above, in this work the Yamashita method (Yamashita et al., 1970) was employed, a well-known slow evaporation route, but with some adjustment in the circuit (controlled air atmosphere, an improved distillation system, and fully isolated from the external environment), which was improved by Junot et al. (2016).

This study is focused on the preparation and investigation of TL and OSL properties of $CaSO_4$:Mn synthesized by the slow evaporation route, since the production route used by our research group showed efficiency in the growth of other crystals, such as $CaSO_4$:Tb,Eu (Junot et al., 2016), $CaSO_4$:Tm and $CaSO_4$:Tm,Ag (Junot et al., 2019), $CaSO_4$:Tb, $CaSO_4$:Tb, Ag and $CaSO_4$:Tb,Ag(NP) (Silva et al., 2020) and $CaSO_4$:Mn,Tb (Silva et al., 2022).

2. Materials and methods

2.1. Sample preparation

The $CaSO_4$:Mn crystals were prepared using a slow evaporation method from a mixture of calcium carbonate ($CaCO_3$) (Merck, 99%), sulfuric acid (H_2SO_4) (Vetec, 95–99%) and manganese nitrate ($Mn(NO_3)_2.4H_2O$) with a concentration value of 0.1 mol%. The parameters to obtain $CaSO_4$:Mn crystals were established in previous works (Junot et al., 2016, 2019; Silva et al., 2020).

After the sulfuric acid evaporation, the $CaSO_4$:Mn crystals were washed, ground, and sieved. The resulting powder was calcined for 1 h at 600 °C. Thereafter, the powder was mixed uniformly with polytetrafluoroethylene (Teflon), in a proportion of 2:1. After a uniaxial pressure of 0.5 tons during 10 s, pellets of (40 ± 1) mg, 6 mm in diameter and approximately 1 mm thickness were produced. Finally, the pellets were sintered at 450 °C for 1 h.

2.2. Sample characterization

X-ray diffraction (XRD) pattern was recorded using Cu-target (Cu-K_α = 1.54 Å) on Rigaku diffractometer (RINT, 2000/PC). The phase identification was performed using the International Center for Diffraction Data (ICDD) PDF 00-037-1496. Scanning electron microscopy (SEM) images were recorded using a Hitachi TM-3000 scanning microscope with carbon substrate. The excitation and emission spectra were obtained using a JASCO FP8600 spectrofluorometer. The thermal behavior was investigated using thermogravimetric analysis (TGA) with a type Shimadzu-50 instrument, at a heating rate of 10 °C/min with N_2 as a carrier gas at a flow rate of 50 cm^3/min.

TL and OSL measurements were carried out using a Risø TL/OSL-DA-20 automatic Reader. The samples were irradiated with a beta source (dose rate of 81.6 mGy/s), which is coupled to the Riso system. In order to carry out measurements of the TL emission spectra, a high resolution spectrometer from Ocean Optics was coupled in place of the photomultiplier. Optical filters used for TL detection were Schott BG-39 and Hoya U-340, and for OSL, Hoya U-340. For the analysis of the heating rate on the TL emission, the pellets were exposed to heating rates varying from 1 °C/s up to 10 °C/s, to a maximum temperature of 400 °C. For all other measurements, the heating rate was kept at 10 °C/s. Glow curve deconvolutions and TL kinetic parameters were obtained by means of OriginLab 8.0 software (OriginLab Co., USA). The TL curve was fitted using the equation for the general kinetic order presented by Chen and McKeever (1997), to determine the kinetic order (b), activation energy (E) and frequency factor (s) parameters of the TL peaks.

In the TL sensitivity analysis, five commercial dosimeters were used for comparison with $CaSO_4$:Mn: $CaSO_4$:Dy (produced at the Dosimetric Materials Laboratory of IPEN), LiF:Mg,Ti (Harshaw TLD-100), CaF_2:Dy (Harshaw TLD-200), CaF_2:Mn (Harshaw TLD-400) and $CaSO_4$:Dy (Harshaw TLD-900). All the pellets were pre-irradiated to 169 mGy with a beta radiation source ($^{90}Sr/^{90}Y$) and the glow curves read immediately using Hoya U-340 (340 ± 40) nm filter.

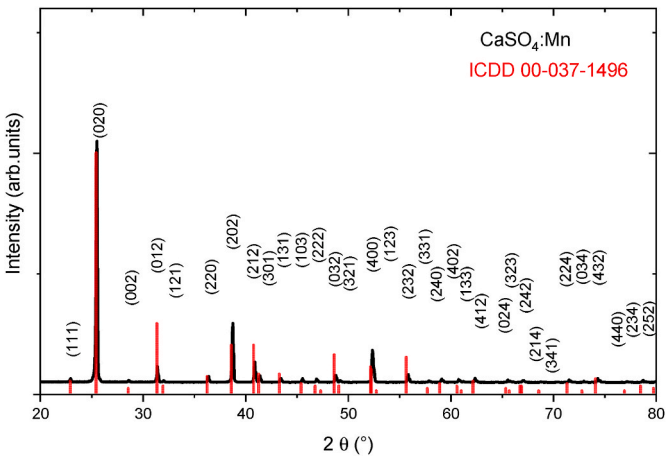

Fig. 1. Experimental X-ray diffractogram of $CaSO_4$:Mn powder, presented with its crystallographic pattern and standard Bragg reflections.

Gamma-^{60}Co irradiations using a 383.65 Gy/h dose rate of GammaCell 220 irradiator and ray unit, Pantak/Seifert, model ISOVOLT 160-HS with beams of average energy of 34 keV (RQR5) were also used to carried out the irradiations for TL measurements.

For the OSL readings, the signal was collected over 40 s and the samples were stimulated with blue LEDs (with emission at 470 nm), in continuous-wave mode. The experimental OSL decay curves composed by three first-order exponential decay functions were obtained by fitting using the following Equation (1):

$$I_{OSL} = A_1\, e^{-t/\tau_1} + A_2\, e^{-t/\tau_2} + A_3\, e^{-t/\tau_3} \quad (1)$$

where I_{OSL} is the total OSL intensity; A_1, A_2, and A_3 are constant coefficients and τ_1, τ_2, and τ_3 are the decay constants related to the different sets of traps (Valença et al., 2018).

The minimum detectable dose (MDD) of the luminescent signal of the produced samples was calculated by Equation (2) proposed by Oberhofer e Scharmann (1981).

$$MDD = (\overline{B} + 3\sigma_{\overline{B}})f_c \quad (2)$$

Where $\overline{B}$ is the average of the TL or OSL response of the non-irradiated dosimeters, $\sigma_{\overline{B}}$ is the standard deviation of the readings of non-irradiated dosimeters, and f_c is a calibration factor calculated from the inverse of the slope of the line of TL/OSL response to absorbed dose. After the TL/OSL measurements, the pellets were thermally treated at 400 °C for 2 h, for reutilization.

3. results and discussion

3.1. Structural characterization

Fig. 1 shows the XRD pattern of synthesized $CaSO_4$:Mn samples. As can be seen, the diffraction peaks agree with those of $CaSO_4$ anhydrite (ICDD 00-037-1496) pattern to a crystal of orthorhombic symmetry (Silva et al., 2021), whose reference lines are included for comparison. The results revealed that the obtained samples showed pure phase and there is no evidence of presence of the dopants due to their low concentrations (≤0.1% mol).

3.2. Scanning electron microscopy (SEM)

The main features on the surface of crystalline $CaSO_4$:Mn are depicted in the SEM micrograph in Fig. 2. The $CaSO_4$ samples obtained after calcination of the compound show well grained images with quite

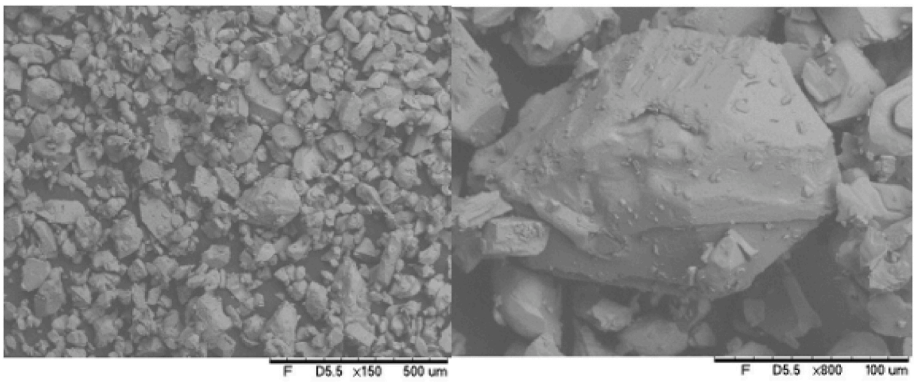

Fig. 2. SEM images of $CaSO_4$:Mn.

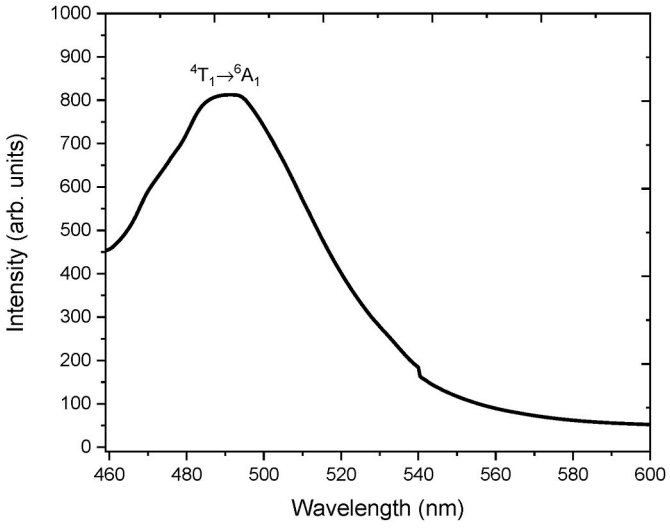

Fig. 3. Emission spectra of $CaSO_4$:Mn excited with 398 nm.

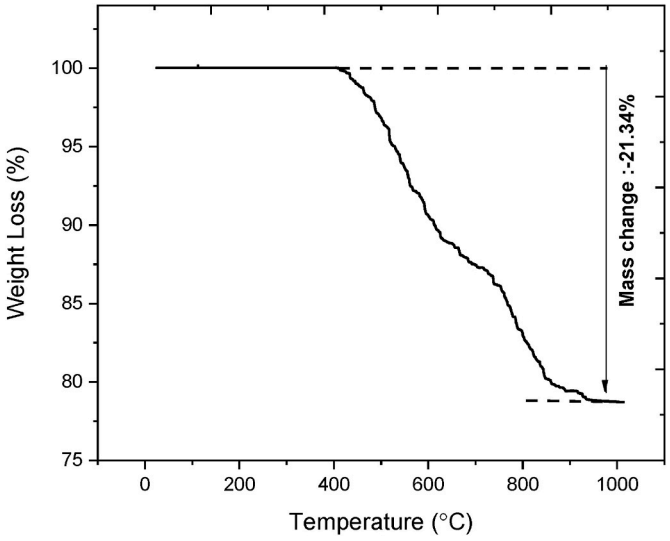

Fig. 4. TGA curves of the as-prepared samples.

agglomeration in the grains with average crystal dimensions of <150 μm.

3.3. Photoluminescence studies

The photoluminescence spectrum of the $CaSO_4$:Mn phosphor is shown in Fig. 3. The spectrum was monitored at an excitation wavelength at 398 nm, showing a broad band around 494 nm, attributable to contributions of Mn^{2+} in the host lattice. The green emission observed is typical for bivalent manganese ions, in four-fold regular tetrahedral coordination, and corresponds to the $^4T_1 \rightarrow {}^6A_1$ transition in Mn^{2+} ion (Luchechko et al., 2019; Menon et al., 2005; Zahedifar et al., 2011).

3.4. Thermogravimetric analysis (TGA)

The thermal behaviors of the $CaSO_4$ powder were determined by thermogravimetric analysis (TGA) as shown in Fig. 4. There is a weight loss of only 1% if the samples are annealed up to 450 °C, and a 20.3% further weight loss on annealing up to 1000 °C. This shows that the temperature used for sintering the pellets at 450 °C for 1 h is adequate since there is no major weight loss, indicating an absence of additional structural changes in this region.

3.5. Thermoluminescent studies

3.5.1. TL emission spectra

The 3D TL emission spectra of $CaSO_4$:Mn irradiated with 50 Gy are shown in Fig. 5. The glow curve for $CaSO_4$:Mn presented a single peak centered at approximately 150 °C, around 494 nm. The wavelength of the emission is consistent with the literature report for Mn^{2+} íons (Luchechko et al., 2019; Menon et al., 2005; Zahedifar et al., 2011). This observed transition corresponds to the $^6A_1 \rightarrow {}^4T_1$ which confirms the incorporation of the Mn^{2+} ion into the calcium sulphate matrix.

Once the peak wavelength is determined, the TL peak for the $CaSO_4$:Mn produced by the evaporation route was found to appear around 150 °C. This showed a large advantage of this material in comparison to the $CaSO_4$:Mn materials reported in the literature, since higher temperature peaks seems to be more stable than lower temperature ones. It is worth mentioning that there is a divergence in the TL emission curve when samples are produced by different synthesis methods. Examples of this variation were reported by Bahl et al. (2017). They obtained by the recrystallization method one glow curve for the $CaSO_4$:Mn with a single peak at around 110 °C. Zahedifar et al. (2011) synthesized this material by the hydrothermal method and they identified one complex glow curve with three overlapping peaks, while by method of Yamashita et al. (1970), this glow curve of $CaSO_4$:Mn presented a simple form and a peak at 100 °C.

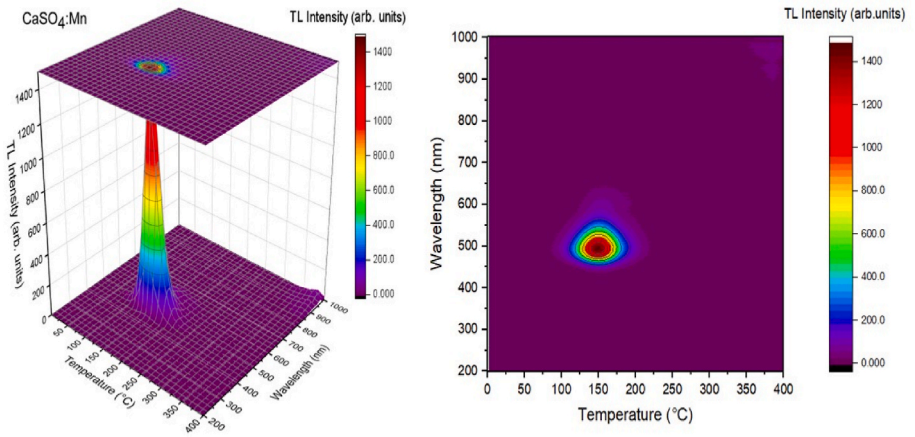

Fig. 5. Isometric 3D-TL emission plot from $CaSO_4$:Mn phosphor. A heating rate of 5 °C/s was used.

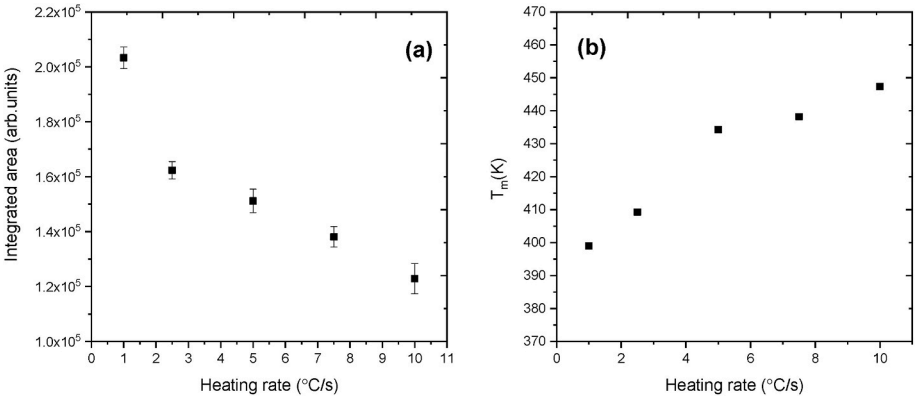

Fig. 6. (a) TL intensity of $CaSO_4$:Mn samples exposed to the same absorbed dose and measured at different heating rates and (b) peak temperatures (T_m) vs. heating rate.

Table 1
Parameters of the TL glow curve of $CaSO_4$:Mn obtained by employing the general kinetic order equation (Chen and McKeever 1997).

Heating rates (°C/s)	T_m (K)	I_m (arb. units)	B (kinetic order)	E (eV)	S (s^{-1})
1.0	399.01 ± 0.36	5434.2 ± 49.68	1.93 ± 0.12	0.83 ± 0.01	$4.69x10^{11}$
2.5	409.24 ± 0.20	4651.77 ± 38.55	1.95 ± 0.03	0.914 ± 0.01	$2.93x10^{12}$
5	434.26 ± 0.20	4100.27 ± 38.56	1.96 ± 0.04	0.97 ± 0.02	$2.84x10^{12}$
7.5	438.20 ± 0.19	3946.37 ± 19.72	1.97 ± 0.03	1.01 ± 0.01	$6.69x10^{12}$
10	447.32 ± 0.15	3541.6 ± 19.21	1.98 ± 0.03	1.07 ± 0.01	$1.86x10^{13}$

3.5.2. *Variation in the heating rate*

The effect of the heating rate on the thermoluminescence of the $CaSO_4$:Mn phosphors was examined. Fig. 6(a) shows TL responses of the samples readout at different heating rates after being irradiated with 169 mGy of a $^{90}Sr/^{90}Y$ beta source. Increasing the heating rate of the sample from 1.0 °C/s to 10 °C/s a TL peak shift to higher temperatures was observed, Fig. 6(b), as well as a decrease of the peak height. This observation may be explained based on the phenomenon of thermal quenching, which takes place inside the phosphor and causes the decrease of luminescence efficiency due to the increased probability of non-radiative transitions (Kadari and Kadri 2015).

Table 1 shows the TL parameters obtained by employing the general kinetic order fitting on TL glow curves of $CaSO_4$:Mn for different heating rates. The peak temperatures (T_m), the maximum peak intensities (I_m), the kinetic order value (b), the activation energies (E) and the frequency factor (s) were determined.

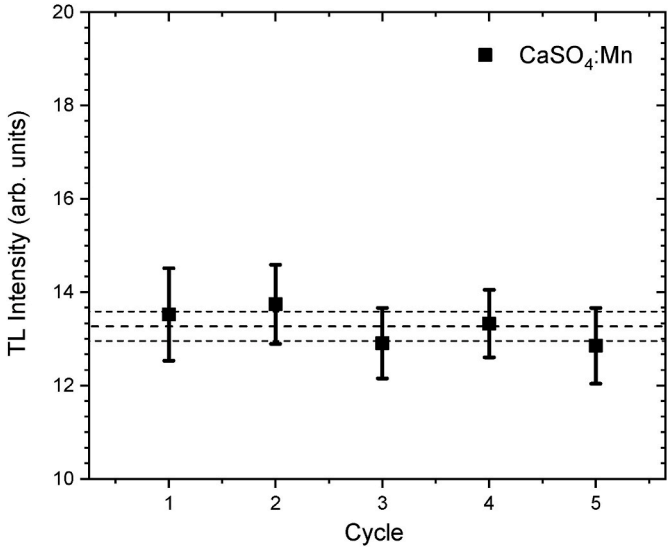

Fig. 7. TL reproducibility of the $CaSO_4$:Mn samples after five cycles of the annealing - irradiation - reading procedure.

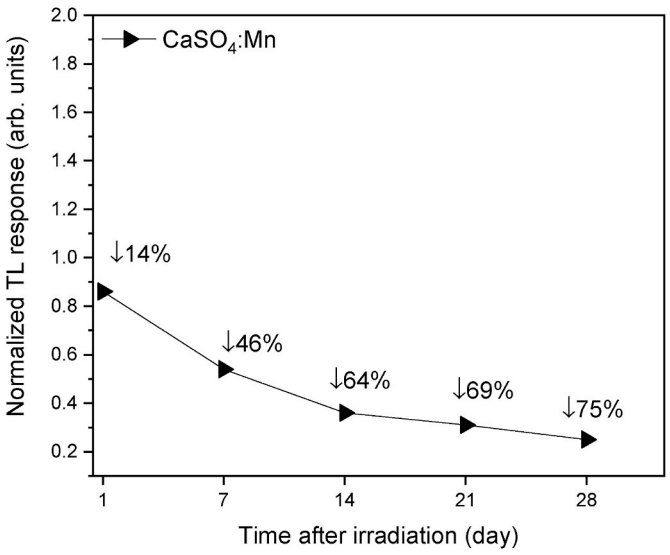

Fig. 8. Normalized TL response of $CaSO_4$:Mn samples, presented with fading percentage in different storage time intervals, after a previous irradiation with 169 mGy ($^{90}Sr/^{90}Y$).

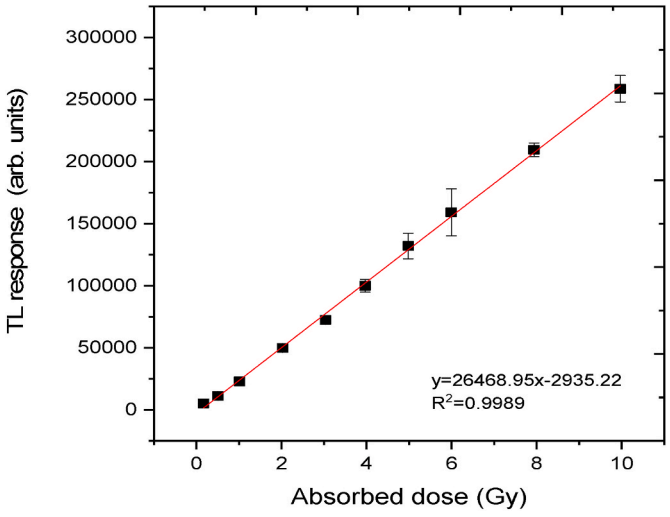

Fig. 9. TL response versus absorbed dose of beta radiation ($^{90}Sr/^{90}Y$).

The TL emission glow curves for the $CaSO_4$:Mn samples showed one peak varying between 399 K and 447 K for different heating rates. The trapping centers located between 0.83 and 1.07 eV were revealed. The order of kinetics was found to be between one and two, indicating the existence of a general order of kinetics in the TL process.

Since a heating rate of 10 °C/s is usually employed in standard dosimetry, in this work it is preferred to maintain this heating rate for all the consecutive TL dosimetric characterizations.

3.5.3. TL reproducibility, fading and linearity

In order to evaluate whether the luminescence signal of the $CaSO_4$:Mn pellets is reproducible, five cycles of annealing - irradiation with 169 mGy - reading were performed. As observed in Fig. 7, the results show an adequate reproducibility, with the average value of the coefficient of 6.22% for $CaSO_4$:Mn samples, meeting the requirements of the ISO 12794 (ISO 2000), which states that this C.V% should not exceed 10%. Hence, the result confirmed that these pellets may be reusable in systemic radiation dose assessment.

The ratio of the TL response of each dosimeter to the mean batch response of all dosimeters results in the homogeneity coefficient (C_H%), and the average value of 3.15% was obtained.

The fading of this phosphor was evaluated up to 28 days after irradiation. Fig. 8 shows normalized TL of the pellets, previously irradiated with 169 mGy, and then being stored over a period of one day, 7 days, 14 days, 21 days and 28 days at room temperature and under light protection. The total integrated area of the glow curves exhibited the following reduction of its original value: 14% in 1 day, 46% in 7 days, 64% in 14 days, 69% in 21 days and 75% after 30 days.

The $CaSO_4$:Mn prepared using slow evaporation route minimized the fading behavior, when compared to those reported in the literature. Bahl et al. (2017) and Menon et al. (2005) reported a fading of the TL intensity of this material very considerable of 40–85% in the first 3 days after radiation exposure. This peak shift to 150 °C in comparison to the 100 °C peak reported, evidences the existence of more deep trap (electrons or holes trapped at deep localized trap states) and stable traps at all levels.

The dose-response curve of the $CaSO_4$:Mn pellets irradiated with absorbed doses from 169 mGy up to 9.971 Gy is shown in Fig. 9. The linear relationship between the TL response and the absorbed doses can be observed in the whole tested dose range. The linear regression for the curve has an R-squared of 0.9989.

3.5.4. TL sensitivity

Fig. 10(a) presents the TL sensitivity described through the TL signals intensity, per unit mass and per unit of absorbed dose ($TL*mg^{-1}*Gy^{-1}$), of the $CaSO_4$:Mn pellets produced in the present work were compared with those of the commercial dosimeters TLD-100 (LiF:Mg,Ti), TLD-200 (CaF_2:Dy), TLD-400 (CaF_2:Mn), TLD-900 ($CaSO_4$:Dy), and $CaSO_4$:Dy

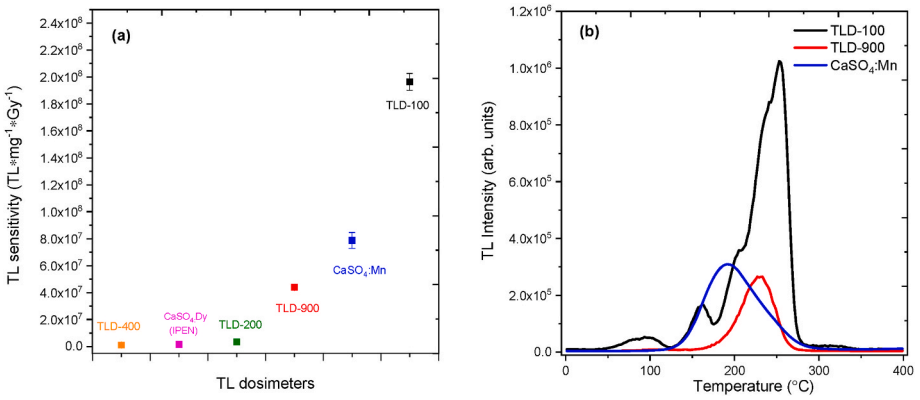

Fig. 10. (a) TL sensitivity of the $CaSO_4$:Mn samples and of commercial dosimeters irradiated with 169 mGy; and (b) TL glow curve of the $CaSO_4$:Mn samples, TLD-100 and TLD-900.

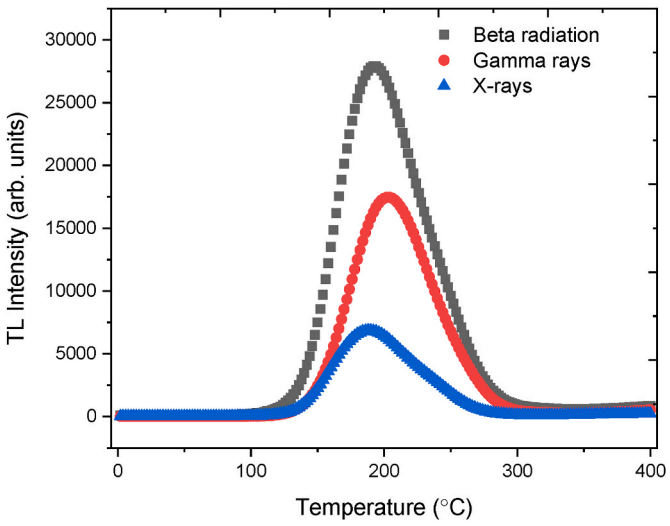

Fig. 11. TL glow curve of $CaSO_4$:Mn samples registered after irradiation with 1 Gy of X (34 keV), β and γ rays.

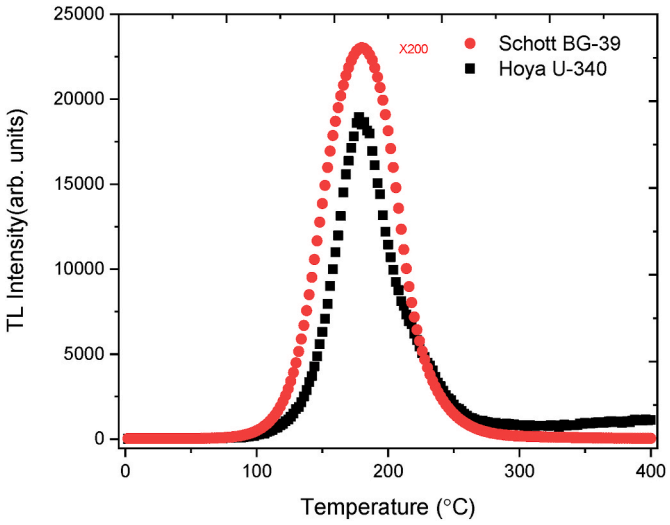

Fig. 12. TL emissions of $CaSO_4$:Mn using Hoya U-340 and Schott BG-39 optical filters.

(IPEN) after being irradiated with absorbed doses of 169 mGy. The results indicate that the TL sensitivity of $CaSO_4$:Mn pellets was 73.7 times higher than that of TLD-400, 49.9 times higher than that of $CaSO_4$:Dy (IPEN), 23.1 times higher than that of TLD-200 and 1.79 times higher than that of TLD-900 measured in similar conditions and using Hoya U-340 (340 ± 40) nm filter. Nevertheless, this sensitivity is still lower than that usually found for high sensitivity TLD material such as TLD-100 (LiF:Mg,Ti).

The analysis of the luminescent sensitivity of a material is a crucial part of the investigation of its dosimetric characteristics (Oberhofer and Scharmann, 1993). For this analysis, comparisons are made with the sensitivities of well-established luminescent dosimeters. A comparison between the TL curves of the $CaSO_4$:Mn samples and those of TLD-100 and TLD-900, which are commercially available, confirms that the $CaSO_4$:Mn studied in this work is useful for radiation dosimetry.

3.5.5. *Effect of ionization radiation: β ($^{90}Sr/^{90}Y$), γ (^{60}Co) and X rays*

In Fig. 11 are shown the typical TL glow curves of $CaSO_4$:Mn samples irradiated with 1 Gy from X (34 keV), β ($^{90}Sr/^{90}Y$) and γ (^{60}Co) ray sources. The TL peak occurs at the same temperature region, but with

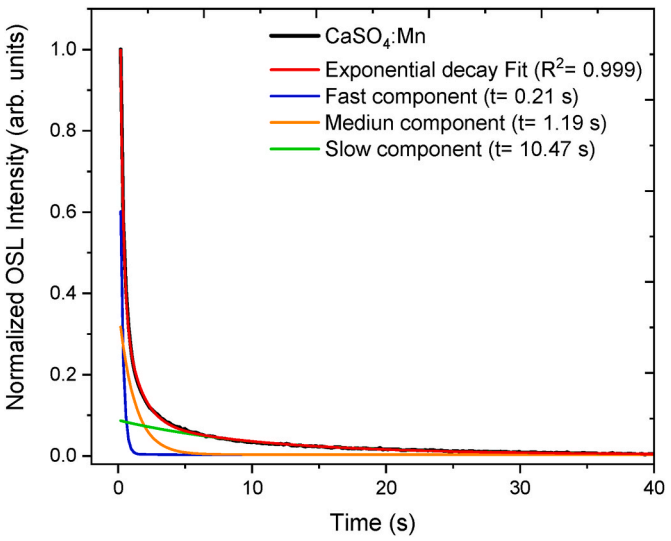

Fig. 13. The CW-OSL curve and fitted OSL decay curves for samples irradiated with 169 mGy ($^{90}Sr+^{90}Y$).

Table 2
The OSL parameters of the exponential fitted curves of the produced compound.

CW-OSL Component	Coefficient A_i	Decay constant t_i (s)	Exponential Fit
Fast	1.527 ± 0.014 (A_1)	0.21 ± 0.01 (t_1)	R^2: 0.9995
Medium	0.371 ± 0.009(A_2)	1.19 ± 0.02 (t_2)	
Slow	0.085 ± 0.001 (A_3)	10.47 ± 0.17 (t_3)	

different intensities. As observed, the peak is more intense for the glow curve irradiated with the $^{90}Sr/^{90}Y$ source, while the lowest intensity was exhibited by the sample exposed to the X source.

Due to its effective atomic number (Z_{eff} = 15.3), which is relatively higher compared to that of soft tissue (Z_{eff} = 7.4), it is expected that the luminescent emission of $CaSO_4$ based dosimeters has sensitivity dependent on the energy and type of the incident radiation (Forner et al., 2020). This behaviour was also confirmed in this work, where it was observed that the TL emission of the samples irradiated with photons is less intense. The TL emission of the samples irradiated with ^{60}Co is more intense than that of samples irradiated with the same dose of X-rays. Similarly, the TL emission of the samples irradiated with beta radiation differs from those irradiated with photon beams.

3.5.6. *TL response with different optical filter*

In this part of the study, TL emissions were measured using a 7.5 mm Hoya U-340 optical filter (290–370 nm). Additionally, TL response measurements were also performed using a Schott BG-39 (330–620 nm) filter for comparison purposes. It is known that $CaSO_4$:Mn emits mainly in the visible of blue and green spectral ranges. As shown in Fig. 12, by changing the filter the TL intensities are altered, but no other changes are induced in the shape nor in temperature range of the TL peak, as mentioned in Section 2.3. TL intensity change is depending on the transmission in the different wavelength region of the optical filter. The TL intensity is about 200 times more intense for the Schott BG-39 filters when compared to the Hoya U-340 filter.

3.6. *Optically stimulated luminescence studies*

3.6.1. *OSL decay curves*

Fig. 13 illustrates a fitting of the OSL decay curve obtained after 169 mGy of beta radiation dose. For this analysis, the samples were

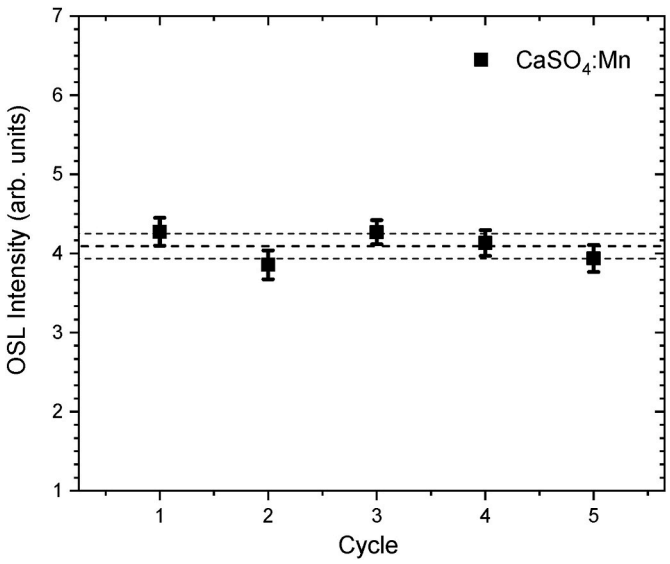

Fig. 14. OSL Reproducibility of the $CaSO_4$:Mn samples after five cycles of the annealing - irradiation - reading procedure.

stimulated with blue light for 40 s. These exponential curves are composed of fast (blue curve), medium (orange curve) and slow (green curve) decay components. The sum of the components (red curve) is very close to the experimental OSL curve (black curve). For this was used to fitted with decaying exponential functions of Eq. (1).

The values of the constant coefficients and decay constants for each of the components are listed in Table 2. In the dose range investigated, the curves present yielded three time constants. As presented in Table 2, the high value of A_1 confirms the predominance of a fast decay component in the experimental OSL decay curve; in this case, the emission of photons results in direct recombination between the electrons in the conduction band and the holes in the valence band of phosphor. The low value of $A_3 = 0.085$ indicates that the significance of the slow component ($\tau_3 = 10.47$) is minimal in the experimental OSL decay curve.

3.6.2. OSL reproducibility

In the present study, the OSL response reproducibility of the $CaSO_4$:Mn pellets was also determined as described in Section 3.4.1 for the TL. In Fig. 14 each point represents the average values of the OSL readings of 15 pellets, and the bars represent their standard deviations. The reproducibility of the OSL measurements was found to be approximately 4.14%, and for the homogeneity study, the homogeneity coefficient (C_H%) the mean value of 4.46% was obtained.

3.6.3. OSL dose response

Fig. 15 (a) shows the OSL decay of $CaSO_4$:Mn samples exposed to the beta source from 169 mGy up to 9.971 Gy. The OSL dose-response curve is shown in Fig. 15 (b). The results showed that the OSL signal is proportional to the absorbed radiation dose, i.e., it increases with the number of trapped electrons and holes. A linear adjustment presented a linear correlation coefficient of 0.9989.

3.6.4. OSL fading

Fig. 16 shows the OSL signal fading behavior of the $CaSO_4$:Mn sample. The fading test was carried out by exposing several pellets to 169 mGy of beta radiation. The signal loss obtained of 63.6% is given by the ratio between the OSL signal from the stored sample (after 28 days) and the signal from the same pellets read immediately after irradiation. The samples exhibited a strong fading, but well below TL fading.

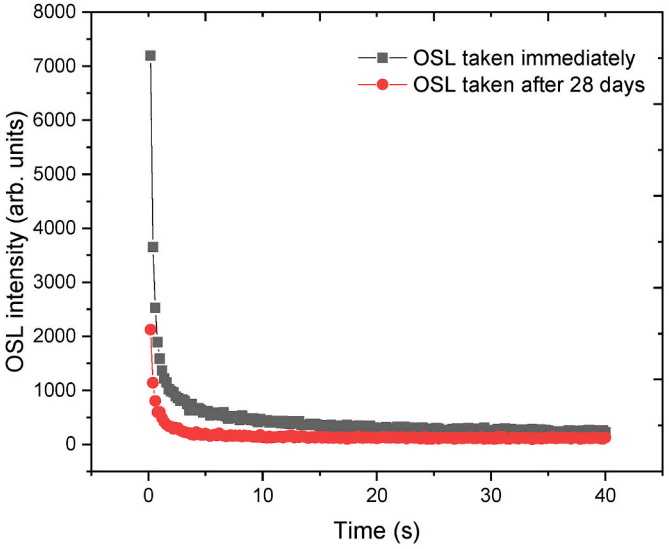

Fig. 16. OSL decay curve for $CaSO_4$:Mn samples, read immediately after irradiation at 169 mGy and after 28 days.

Table 3
MDD values for $CaSO_4$:Mn and their uncertainties for the TL and OSL techniques.

Luminescent technique	$\overline{B}$ (arb. units)	$\sigma_{\overline{B}}$ (arb. units)	f_c (mGy/arb. units)	MDD (mGy)
TL	**2414.3**	**287.4**	**0.0015**	**4.95 ± 0.03**
OSL	**6767.5**	**100.7**	**0.0268**	**189.83 ± 0.09**

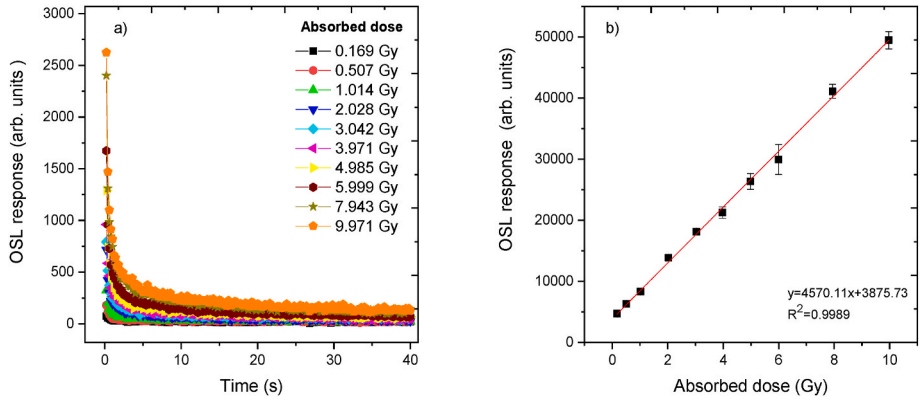

Fig. 15. (a) The OSL response of the samples of $CaSO_4$:Mn and (b) as a function of the absorbed dose of beta radiation ($^{90}Sr/^{90}Y$).

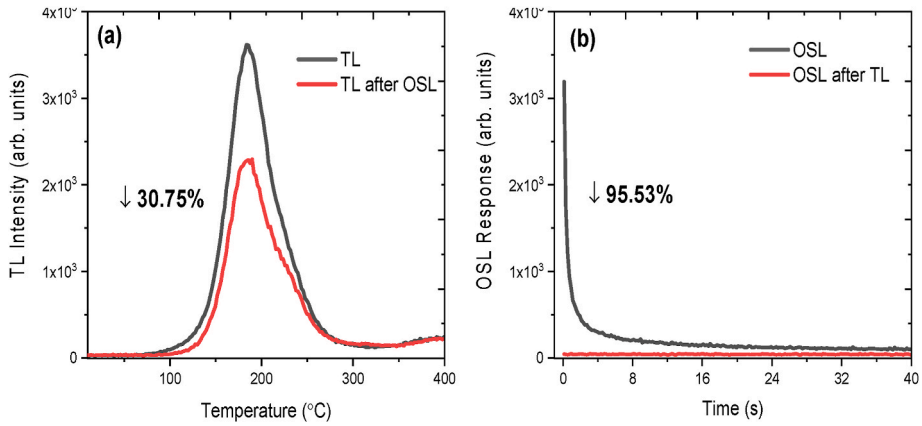

Fig. 17. Correlation between the TL and OSL emissions of the $CaSO_4$:Mn samples (a) obtained from consecutive luminescent measurements TL→ OSL and (b) OSL → TL.

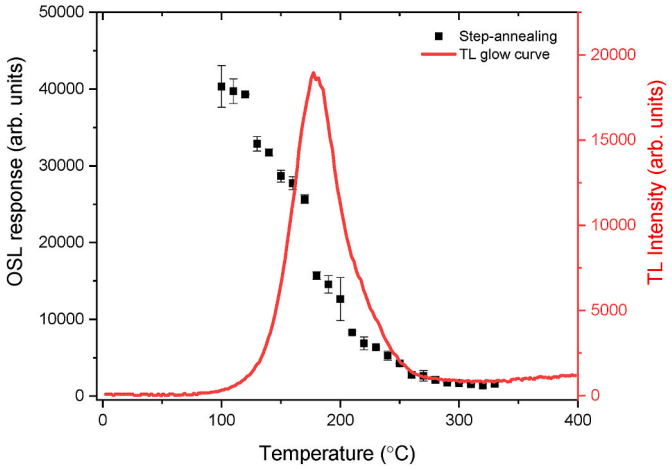

Fig. 18. OSL response (integrated area) of $CaSO_4$:Mn samples, after various pre-heating temperatures and its comparison with the TL glow curve.

3.6.5. *Minimum detectable dose*

The minimum detectable dose (MDD) of $CaSO_4$:Mn pellets was estimated by calculating the average and standard deviation of the TL/OSL signal of the samples treated at 400 °C for 1 h and those not irradiated. As shown in Table 3, the values obtained for the minimum detectable dose were: 4.95 mGy and 189.8 mGy for TL technique and OSL technique, respectively. The estimated value of its MDD is important in low dose measurements where the dosimeter signal is almost equal to the background signal.

3.6.6. *Correlation between the TL and OSL emissions*

Fig. 17 (a) shows the TL glow curve of the $CaSO_4$:Mn samples without previous OSL stimulation (black line) and TL with previous OSL stimulation (red line). The previous OSL measurements of the samples significantly reduced the TL signal, by approximately 30.75%. In this case, it is correct to affirm that the OSL signal is correlated to the TL peak. When comparing other materials produced by the slow evaporation route, the $CaSO_4$:Mn presented a TL signal with the lowest photoionization cross section in relation to $CaSO_4$:Tm and $CaSO_4$:Tm,Ag (Junot et al., 2019), $CaSO_4$:Tb (Silva et al., 2020) and $CaSO_4$:Mn,Tb (Silva et al., 2022). For the same photon flux of the light source, a low photoionization cross section of the trap denotes a low probability of release of the trapped electrons after an optical stimulation, which results in a less intense decay of the OSL signal (Valença et al., 2018).

Fig. 17 (b) shows the OSL exponential decay without previous TL stimulation (black line) and OSL with previous TL stimulation (red line). It was also observed that the previous TL measurements of the samples significantly reduced the OSL signal, causing the reduction of the OSL signal to background levels. This indicates that the optically active traps are easily emptied by thermal stimulation (Junot et al., 2019).

Step-annealing measurements were also performed to prove the relationship between the light-affected parts of the TL glow curve and the source of the OSL signals (Yukihara, and McKeever 2011). TL and OSL were correlated in order to investigate how OSL traps are affected by the step-by-step emptying of TL traps. The process was performed as follows: (i) the sample was irradiated with a beta dose of 1 Gy at room temperature; (ii) after irradiation, the sample was heated up to a pre-defined temperature (Tstop), at a heating rate of 10 °C/s; (iii) the sample was cooled back to room temperature; and then (iv), the OSL was recorded with 40 s blue light stimulation. Fig. 18 shows the changes of integrated OSL signals versus step annealing temperatures (100 °C–330 °C, with 10 °C intervals), as compared with the TL glow curve.

This data reaffirms that the OSL signal arises mainly from the TL peak centered at 180 °C. The decrease in OSL signal intensity after preheating at 100 °C is due to prior recombination of the electrons responsible for the OSL signal. This reduction is intensified with subsequent heating, until background levels are reached at approximately 280 °C. This proves the decrease in trapped electron density with increasing preheating temperatures. The mechanism involved in the generation of the OSL signal is originated mostly from a single trapping center, at least under the stimulation wavelength used in this measurement (470 nm).

4. Conclusions

Although the $CaSO_4$:Mn has been left out by the scientific community due to its low temperature peak and strong fading of its TL signal, these characteristics can be partially circumvented by applying a suitable preparation method. In this work manganese doped $CaSO_4$ were synthesized by an adaptation of the slow evaporation route, and the obtained powders were calcined at 600 °C for 2 h. The X-ray diffraction analyses showed that the phosphor was efficiently synthesized, since the diffraction peaks agree with those of $CaSO_4$ anhydrite (ICDD 00-037-1496) pattern to a crystal of orthorhombic symmetry. SEM images showed irregular grain morphology with quite agglomeration grains and average crystal dimensions of <150 μm. The results for the PL and TL emission spectra confirmed the presence Mn^{2+} ions in the crystal matrix, once the emission band fits with the characteristic line of the Mn^{2+} emission features, ascribed to the $^6A_1 \rightarrow {}^4T_1$ transition. The thermal behaviors by thermogravimetric analysis (TGA) showed that the temperature used for sintering the pellets at 450 °C for 1 h is adequate since there is an insignificant weight loss. A dosimetric analysis showed that

$CaSO_4$:Mn for different heating rates presented the glow curve with a single typical peak and trapping centers located between 0.83 eV and 1.07 eV. The order of kinetics was found to be between one and two, indicating the existence of a general order of kinetics in the TL process. $CaSO_4$:Mn presented a higher TL sensitivity to radiation than CaF_2:Dy, CaF_2:Mn and $CaSO_4$:Dy. The luminescent emission of $CaSO_4$:Mn has high TL sensitivity to beta radiation dose when compared to gamma and X-ray responses. The samples also showed an adequate OSL decay curve, with a predominance of a fast decay component. All samples presented properties useful for dosimetric purposes, linearity of the luminescent signals, when irradiated with doses between 169 mGy and 10 Gy, good reproducibility, lowest detectable doses for the OSL and TL signals, on the order of mGy; besides that, they present a significantly fading below those reported in the literature. After 28 days, the TL glow curve showed a 75% fading of its original value, and for the OSL decay curve the signal loss obtained was of 63.6%.

CRediT authorship contribution statement

Anderson M.B. Silva: Writing – review & editing, Writing – original draft, VisualizationVisualization, Methodology, Investigation, Formal analysis, Data curation, Conceptualization. **Daniel S. Rodrigues:** Visualization, Investigation. **Patrícia L. Antonio:** Visualization, Investigation. **Danilo O. Junot:** Writing – review & editing, Visualization, Investigation, Data curation, Conceptualization. **Linda V.E. Caldas:** Visualization, Resources, Conceptualization. **Divanizia N. Souza:** Writing – review & editing, Visualization, Supervision, Resources, Project administration.

Declaration of competing interest

The authors declare that they have no known competing financial interests or personal relationships that could have appeared to influence the work reported in this paper.

Data availability

Data will be made available on request.

Acknowledgments

The authors thank the Brazilian agencies Comissão Nacional de Energia Nuclear (CNEN), Coordenação de Aperfeiçoamento de Pessoal de Nível Superior - CAPES (Project 88881.157892/2017–01), Conselho Nacional de Desenvolvimento Científico e Tecnológico - CNPq (Projects: 427010/2016–0, 308090/2016–0, 165609/2020–6, 305142/2021–6, 160306/2019–1 and 466512/2018–5), Fundação de Amparo a Pesquisa do Estado de São Paulo – FAPESP (Project 2018/05982–0) and MultiLab (Multi-User Physics Laboratories) and CLQM (Center of Multi-users Chemistry Laboratories) from Federal University of Sergipe for the analysis support.

References

Bahl, S., Kumar, V., Bihari, R.R., Kumar, P., 2017. Investigations of OSL properties of $CaSO_4$:Mn phosphor exposed to gamma and beta radiations. J. Lumin. 181, 36–43. https://doi.org/10.1016/j.jlumin.2016.09.004.

Chen, R., McKeever, S.W.S., 1997. Theory of Thermoluminescence and Related Phenomena. World Scientific, New Jersey.

Du, A., Du, Q., Liu, X., Yang, Y., Xia, C., Zou, J., Li, J., 2021. Ce: YAG transparent ceramics enabling high luminous efficacy for high-power LEDs/LDs. J. Inorg. Mater. 36 (883) https://doi.org/10.15541/jim20200727.

Forner, L.A., Viccari, C., Nicolucci, P., 2020. Dosimetric properties of thermoluminescent pellets of CaSO4 doped with rare earths at low doses. Radiat. Phys. Chem. 171, 108704.

ISO 12794, 2000. Nuclear Energy–Radiation Protection–Individual Thermoluminescence Dosemeters for Extremities and Eyes. International Organization for Standardization, Geneva.

Junot, D.O., Barros, J.P., Caldas, L.V.E., Souza, D.N., 2016. Thermoluminescent analysis of $CaSO_4$:Tb,Eu crystal powder for dosimetric purposes, Radiat. Meas 90, 228–232. https://doi.org/10.1016/j.radmeas.2016.01.020.

Junot, D.O., Santos, A.G., Antonio, P.L., Rezende, M.V., Souza, D.N., Caldas, L.V.E., 2019. Dosimetric and optical properties of $CaSO_4$: Tm and $CaSO_4$: Tm, Ag crystals produced by a slow evaporation route. J. Lumin. 210, 58–65. https://doi.org/10.1016/j.jlumin.2019.02.005.

Kadari, A., Kadri, D., 2015. New numerical model for thermal quenching mechanism in quartz based on two-stage thermal stimulation of thermoluminescence model. Arab. J. Chem. 8, 798–802. https://doi.org/10.1016/j.arabjc.2013.05.027.

Kadari, A., Mahi, K., Mostefa, R., Badaoui, M., Mameche, A., Kadri, D., 2016. Optical and structural properties of Mn doped CaSO4 powders synthesized by sol-gel process. J. Alloys Compd. 688, 32–36. https://doi.org/10.1016/j.jallcom.2016.07.040.

Lin, S., Lin, H., Ma, C., Cheng, Y., Ye, S., Lin, F., Wang, Y., 2020. High-security-level multi-dimensional optical storage medium: nanostructured glass embedded with LiGa5O8: Mn^{2+} with photostimulated luminescence. Light Sci. Appl. 9, 1–10. https://doi.org/10.1038/s41377-020-0258-3.

Liu, X., Wang, Y., Li, X., Yi, Z., Deng, R., Liang Liu, X., 2017. Binary temporal up conversion codes of Mn^{2+}-activated nanoparticles for multilevel anti-counterfeiting. Nat. Commun. 8, 899. https://doi.org/10.1038/s41467-017-00916-7.

Luchechko, A., Zhydachevskyy, Y., Ubizskii, S., Kravets, O., Popov, A.I., Rogulis, U., A Suchocki, A., 2019. Afterglow, TL and OSL properties of Mn $^{2+}$-doped $ZnGa_2O_4$ phosphor. Sci. Rep. 9, 1–8. https://doi.org/10.1038/s41598-019-45869-7.

Menon, S.N., Sanaye, S.S., Dhabekar, B.S., Kumar, R., Bhatt, B.C., 2005. Role of Mn as a co-dopant in $CaSO_4$: Mn, Pr TL phosphor. Radiat. Meas. 39, 111–114. https://doi.org/10.1016/j.radmeas.2004.06.004.

Nuraeni, N., Kartikasari, D., Yani, S., Hiswara, E., Haryanto, F., Iskandar, F., Waris, A., 2019. Thermoluminescence characteristic of CaSO4: Dy on β and γ radiation. J. Phys. Conf. Ser. 1248, 012081 https://doi.org/10.1088/1742-6596/1248/1/012081.

Oberhofer, M., Scharmann, A., 1981. Applied Thermoluminescence Dosimetry. CRC Press, Ispra.

Oberhofer, M., Scharmann, A., 1993. Techniques and Management of Personnel Thermoluminescence Dosimetry Services. Springer Science & Business Media.

Raghuwanshi, V.S., Harizanova, R., Haas, S., Tatchev, D., Gugov, I., Dewhurst, C., Russel, A., Hoell, A., 2014. Magnetic nanocrystals embedded in silicate glasses studied by polarized SANS. J. Non-Cryst. Solids 385, 24–29. https://doi.org/10.1016/j.jnoncrysol.2013.10.007.

Rani, R.S., Lakshmanan, A.R., Sivakumar, V., Venkatasamy, R., Annalakshmi, O., Jose, M.T., Marimuthu, K.N., 2015. Redox and charge transfer processes and luminescence in $CaSO_4$:Zn,Mn. Radiat. Meas. 76, 1350–4487. https://doi.org/10.1016/j.radmeas.2015.03.001.

Silva, A.M.B., Souza, L.F., Antonio, P.L., Junot, D.O., Caldas, L.V.E., Souza, D.N., 2022. Effects of manganese and terbium on the dosimetric properties of $CaSO_4$. Radiat. Phys. Chem. 198, 110207 https://doi.org/10.1016/j.radphyschem.2022.110207.

Silva, A.M.B., Silveira, W.S., Matos, T.S., Junot, D.O., Rezende, M.V., Souza, D.N., 2021. Effect of terbium and silver co-doping on the enhancement of photoluminescence in $CaSO_4$ phosphors. Opt. Mater. 111, 110717 https://doi.org/10.1016/j.optmat.2020.110717.

Silva, A.M.B., Junot, D.O., Caldas, L.V.E., Souza, D.N., 2020. Structural, optical and dosimetric characterization of $CaSO_4$:Tb, $CaSO_4$:Tb,Ag and $CaSO_4$:Tb,Ag(NP). J. Lumin. 224, 117286 https://doi.org/10.1016/j.jlumin.2020.117286.

Song, E., Ye, S., Liu, T., Du, P., Si, R., Jing, X., Ding, S., Peng, M., Zhang, Q., Wondraczek, L., 2015. Tailored near-infrared photoemission in fluoride perovskites through activator aggregation and super-exchange between divalent manganese ions. Adv. Sci. 2, 1500089 https://doi.org/10.1002/advs.201500089.

Valença, J.V., Silva, A.C., Dantas, N.O., Caldas, L.V., d'Errico, F., Souza, S.O., 2018. Optically stimulated luminescence of the 20Li2CO3 – (X)K2CO3 – (80 -X)B2O3 glass system. J. Lumin. 200, 248–253. https://doi.org/10.1016/j.jlumin.2018.03.060.

Wang, X.J., Xie, R.J., Dierre, B., Takeda, T., Suehiro, T., Hirosaki, N., Sekiguchi, T., Sun, Z., 2014. A novel and high brightness AlN: Mn^{2+} red phosphor for field emission displays. Dalton Trans. 43 (16), 6120–6127. https://doi.org/10.1039/C3DT53532K.

Watanabe, K., 1951. Properties of $CaSO_4$:Mn phosphor under vacuum ultraviolet excitation. Phys. Rev. 83, 785–791. https://doi.org/10.1103/PhysRev.83.78.

Yamashita, T., Sakai, K., Kitamura, S., 1970. Calcium sulfate activated by lead and manganese for thermoluminescence dosimetry. J. Nucl. Sci. (Seoul) 7, 105–110. https://doi.org/10.1080/18811248.1970.9734651.

Yukihara, E.G., McKeever, S.W., 2011. Optically Stimulated Luminescence: Fundamentals and Applications. John Wiley & Sons.

Zahedifar, M., Mehrabi, M., Harooni, S., 2011. Synthesis of $CaSO_4$:Mn nanosheets with high thermoluminescence sensitivity. Appl. Radiat. Isot. 69, 1002–1006. https://doi.org/10.1016/j.apradiso.2011.01.036.

Zhou, C., Song, J., Zhou, L., Zhong, L., J Liu, J., Qi, Y., 2015. Greener synthesis and optimization of highly photoluminescence Mn^{2+}**-doped ZnS quantum dots**. J. Lumin. 158, 176–180. https://doi.org/10.1016/j.jlumin.2014.09.053.